



PONTIFICIA UNIVERSIDAD CATOLICA DE CHILE
ESCUELA DE INGENIERIA

SAR EFFECTS ON EVAPORATION FLUXES FROM SHALLOW GROUNDWATER

VERÓNICA BELÉN FIERRO CORTÉS

Thesis submitted to the Office of Research and Graduate Studies in partial fulfillment of the requirements for the Degree of Master of Science in Engineering

Advisor:

JOSÉ FRANCISCO MUÑOZ P.

Santiago de Chile, (March, 2015)

© 2015, Verónica Fierro Cortés



PONTIFICIA UNIVERSIDAD CATOLICA DE CHILE
ESCUELA DE INGENIERIA

SAR EFFECTS ON EVAPORATION FLUXES FROM SHALLOW GROUNDWATER

VERÓNICA BELÉN FIERRO CORTÉS

Members of the Committee:

JOSÉ FRANCISCO MUÑOZ P.

FRANCISCO SUAREZ P.

MARÍA FERNANDA HERNÁNDEZ L.

SCOTT W. TYLER

GLORIA ARANCIBIA H.

Thesis submitted to the Office of Research and Graduate Studies in partial fulfillment of the requirements for the Degree of Master of Science in Engineering

Santiago de Chile, (March, 2015)

Dedicated to my family for
their constant love and support.

ACKNOWLEDGMENTS

First and foremost, I have to thank my advisor, Professor José F. Muñoz, for his assistance and dedication in every step of this process. I also greatly thank Professor Francisco Suárez, for his guidance and great disposition every time I needed it. Both were essential through the development of my research.

I want to thank to whole team of the Department of Hydraulic and Environmental Engineering, especially to my friends Javiera, Marcela, Paulina, Toya, Edwin and Alex, for their friendship, support and patience during my stay in the office. I also thank my friends of Engineering for their company and great moments during the career.

I also thank the support of CONICYT through the Fondecyt project 1130522 for the provided funds, which made possible the developed of this research.

Most importantly, none of this could have happened without my family. My mom María Cristina and my sister María Paula, who accompanied me and encouraged me to complete my Master. Also to my sister María de los Ángeles and my brother in law Eduardo for their help every time I needed it. And my father Ricardo for his support and love.

TABLE OF CONTENTS

	Page
ACKNOWLEDGMENTS.....	iv
TABLE OF CONTENTS	v
LIST OF TABLES	viii
LIST OF FIGURES.....	ix
ABSTRACT	xi
RESUMEN	xii
1 INTRODUCTION	1
1.1 Evaporation in non-saline soils	1
1.2 Evaporation in saline soils.....	2
1.2.1 Previous investigations	2
1.2.2 SAR index: Sodium adsorption ratio	10
1.3 Hypothesis	12
1.4 Objectives	12
2 THEORY	13
2.1 Liquid water and vapor flow	13
2.2 Heat transport	14
2.3 Surface energy balance.....	15
2.4 Solute transport.....	15

2.4.1	Standard solute transport	16
2.4.2	Equilibrium chemistry	17
3	MATERIALS AND METHODS.....	18
3.1	Determination of soil properties.....	18
3.1.1	Samples preparation.....	18
3.1.2	Hydraulic properties	19
3.1.3	Thermal properties.....	21
3.2	Model simulations	21
3.2.1	Numerical model: HYDRUS 1D	22
3.2.2	Evaporation from soils with different SAR	24
3.2.3	Effect of evaporation on salts concentration.....	26
3.2.4	Effect of soil stratification on evaporation fluxes.....	27
4	RESULTS AND DISCUSSION.....	28
4.1	Soil properties.....	28
4.1.1	Hydraulic properties	28
4.1.2	Thermal properties.....	31
4.2	Model simulations	32
4.2.1	Evaporation from soils with different SAR	32
4.2.2	Effect of evaporation on salts concentration.....	35
4.2.3	Effect of soil stratification on evaporation fluxes.....	36
5	CONCLUSIONS	40

5.1	SAR effect on soil hydraulic properties	40
5.2	SAR effect on evaporation	40
5.3	General conclusions	41
REFERENCES		42

LIST OF TABLES

Table 3-1: Ionic solutions composition.....	18
Table 3-2: Solute transport and reaction parameters used on numerical simulation.	26
Table 4-1: Soil water retention parameters obtained by using the van Genuchten's equation (1980).	30
Table 4-2: Hydraulic conductivity for three soils with different SAR. Results indicate no significant differences between these three soils.	30
Table 4-3: Chung and Horton parameters and fitted coefficient.....	31
Table 4-4: Cumulative evaporation after 60 days for different scenarios; two soils with different SAR and four water table levels. Differences between the two soils increase when the water table gets deeper.	35

LIST OF FIGURES

Figure 1-1: Results obtained by Hernandez-López et al. 2014 a) Observed (points) and estimated (line) water retention curve for original soil sample, b) observed (points) and simulated (line) water content profile after evaporation using SiSPAT model, c) Estimated water retention curves defined for stratified soil and d) observed and simulated water content profile using stratification.	4
Figure 1-2: Experimental and simulated results of the evaporation rate from a saline soil. Numerical estimations improve when evaporation resistance of a salt crust at surface is considered (Modified from Fujimaki et al., 2006).....	5
Figure 1-3: Cumulative evaporation in sand (left) and silt columns (right) with different salts types and concentrations. In both cases, evaporation is higher for lower salt concentrations (Gran et al, 2011).	7
Figure 1-4: Water content, concentration and temperature profiles at the end of the halite experiment. Salt concentration increase at the surface, decreasing volumetric water content at this zone (Modified from Gran et al., 2011).....	7
Figure 1-5: a) Change of the location of the vaporization plane; and b) Change of the evaporation rate and soil salt depth on soil surface. Vaporization plane decreases according to saturation. (Modified from Zhang et al., 2014).....	9
Figure 1-6: a) Water retention curves for loam. b) Cumulative evaporation for loam with three different models (Ciocca et al., 2014).	10
Figure 3-1: Experimental setup - Water retention curve.....	19
Figure 3-2: Experimental setup - Constant head permeameter.....	20
Figure 3-3: Experimental setup to determine the thermal properties as a function of soil water content.	21
Figure 3-4: Conceptual model.....	25
Figure 3-5: Conceptual model for a stratified soil.	27

Figure 4-1: Observed (points) and estimated (lines) water retention curve for saline soils with different SAR. Results indicate that an increase in the SAR increases the water retention capacity of the soil for a fixed pressure.29

Figure 4-2: Thermal conductivity curve. Measured (points) and estimated (line) thermal conductivities for different water content values.31

Figure 4-3: Estimated cumulative evaporation for three soils with different SAR after 60 days of simulation. A soil with higher SAR presents higher cumulative evaporation than other soils with lower SAR index.33

Figure 4-4: Water content profile for three soils with different SAR after 60 days. The soil with higher SAR presents a wetter profile than the other soils under the same conditions.34

Figure 4-5: SAR index distribution after 7 days of simulation. The SAR index increases near the surface as a result of evaporation fluxes.36

Figure 4-6: SAR distribution for the stratified soil.37

Figure 4-7: Estimated cumulative evaporation for a uniform and stratified soil. The stratified soil presents greater evaporation than the uniform soil.38

Figure 4-8: Cumulative evaporation as a function of the first layer thickness of a stratified soil after 60 days of simulation (points). The dashed lines indicate the cumulative evaporation for a uniform soil with SAR 3.73 (green) and 5.4 (red). When the first layer thickness increases, evaporation from the stratified soil is similar to a uniform soil with the same SAR of first layer.39

ABSTRACT

Saline soils are common in arid zones, where evaporation from shallow groundwater is generally the major component of the water balance. Thus, to correctly manage the water resources in these zones, it is important to quantify the evaporation fluxes. Evaporation from saline soils is a complex process that couples the movement of salts, heat, liquid water and water vapor, and strongly depends on the soil water content. Precipitation/dissolution reactions can change the soil structure and alter flow paths, modifying evaporation flows. In this research, the effect of sodium adsorption ratio (SAR) on soil hydraulic properties was evaluated experimentally. HYDRUS-1D was used to represent the movement of liquid water and water vapor in a saline soil column using experimental results. To determine the effect of SAR on evaporation fluxes, soils with different SAR were used in numerical simulations. It was found that for higher sodium concentrations, the soil increase its water retention capacity, increasing the cumulative evaporation. Also, it was found that evaporation fluxes increase salt concentration in the region near the soil surface, changing the soil's water retention capacity in those zones. Then, the movement of salts causes differences in evaporation fluxes. It is thus necessary to incorporate salt precipitation/dissolution and its effects on the retention curve to correctly simulate evaporation in saline soils.

Keywords: Water retention curve, evaporation, saline soils, sodium adsorption ratio.

RESUMEN

Comúnmente, los suelos salinos están presentes en zonas áridas, donde la evaporación desde napas subterráneas someras es uno de los componentes principales del balance hídrico. Así, para un correcto manejo del recurso hídrico de esas zonas, es importante cuantificar los flujos de evaporación. La evaporación en suelos salinos es un proceso complejo que incluye el movimiento de solutos, calor, agua líquida y vapor de agua, y depende directamente del contenido de agua del suelo. Las reacciones de precipitación o disolución de solutos pueden cambiar la estructura del suelo y alterar los patrones de flujo, modificando los flujos de evaporación. En este trabajo se evaluó experimentalmente el efecto de la relación de adsorción de sodio (RAS) en las propiedades hidráulicas del suelo; curvas de retención, $\theta(h)$, y de conductividad hidráulica, $K(h)$. Además, se usó el modelo HYDRUS-1D para representar el movimiento de agua líquida y vapor de agua en una columna de suelo salino usando los resultados experimentales. Para determinar el efecto del RAS en los flujos de evaporación, se simuló el proceso de evaporación en suelos con distinto RAS. Se encontró que un aumento en el RAS aumenta la capacidad de retención de agua del suelo y también aumenta su evaporación acumulada. Además, se determinó que los flujos de evaporación producen un aumento de las concentraciones de sal en la zona cercana a la superficie, cambiando la capacidad de retención de agua del suelo en esa zona. Este transporte de sales también causa diferencias en los flujos de evaporación. Así, para una correcta simulación del proceso de evaporación en suelos salinos, es necesario incorporar reacciones de precipitación/disolución y su efecto en la curva de retención del suelo.

Palabras clave: Curva de succión, evaporación, suelos salinos, relación de adsorción de sodio.

1 INTRODUCTION

Arid zones cover more than 40% of the earth surface (Salas, 2000). In closed basins, such those occurring in the north of Chile, evaporation is the main water discharge from the aquifer (Ullman, 1985; Saito et al., 2006, Shah et al., 2007). Thus, to estimate the water balance in these zones, a correct quantification of the evaporation fluxes is necessary. In arid zones, evaporation fluxes cause salts transport modifying soil salinity (Rengasamy & Olsson, 1991; Zhang et al., 2014).

Evaporation from non-saline and saline soils has been studied in recent years, mainly because of its influence on agricultural processes and water availability (Saito et al., 2006; Han et al., 2013).

1.1 Evaporation in non-saline soils

Evaporation from bare soils in absence of salts has been widely studied (Boulet et al., 1997; Assouline et al., 2008; Bittelli et al., 2008). It is a complex process that couples water and vapor flow, and heat transport (Kondo et al., 1990; Bittelli et al., 2008). Evaporation requires three conditions to occur within a soil system: 1) an energy supply; 2) a vapor pressure gradient in the atmosphere-soil interface; and 3) water availability from the ground (Qiu and Ben-Asher, 2010).

Evaporation rates depend on soil saturation and three stages of evaporation can be identified (Gardner and Hillel, 1962; Idso et al., 1974). The first stage occurs when the soil is saturated, where the evaporation rate is large and near to the potential evaporation. In this stage, the evaporation rate is controlled by atmospheric conditions such as air temperature, solar radiation, wind speed and relative humidity (Penman, 1948). When the soil is unsaturated, such as in arid zones, there are two other stages. The second stage occurs when the soil is still moist. At this stage, the evaporation rate gradually decreases and it is controlled by both atmospheric and soil hydraulic

conditions. The third stage occurs when the soil is almost at its driest state. In this stage, evaporation is very low and controlled by soil physical characteristics (Qiu and Ben-Asher, 2010) and vapor diffusion. In both second and third stages evaporation is influenced by the water table depth (Rose et al., 2005). In second and third stages, an evaporation front is observed. The evaporation front is defined as a liquid-vapor discontinuity that divides the zone of the profile where liquid water flows and another zone where only vapor flows (Boulet et al., 1997).

1.2 Evaporation in saline soils

Evaporation from saline soils has also been widely studied in the last years (Ullman, 1985; Nassar & Horton, 1999; Johnson et al., 2010). The main difference compared to evaporation from non-saline soils is that now it is necessary include solute transport (Xue and Akae, 2010; Gran et al., 2011). In saline soils salts can be dissolved in the solution or precipitated in the soil matrix, and its presence in the system has an impact on evaporation fluxes (Fujimaki et al., 2006; Zhang et al., 2014).

1.2.1 Previous investigations

Many authors have studied the evaporation process in saline soils using laboratory experiments to represent the behavior of soils under controlled meteorological conditions (Fujimaki et al. 2006; Gran et al., 2011; Hernández-López, 2014). A general observation reported is that salts concentrates at the soil surface, as is commonly found in nature.

Hernández-López et al. (2014) made an evaporation experiment using a soil column with a constant water table level. They used a soil sample extracted from the salar del Huasco basin in the Primera región de Tarapacá, Chile. Before the experiment, they experimentally determined the soil hydraulic properties (water retention curve and saturated hydraulic conductivity) and fitted the van Genuchten (1980) model to the

observed data (Figure 1-1a). Then, they supplied energy to the top of the soil column using an infrared lamp, which represented solar radiation. At the same time, they kept a constant water table with a Mariotte tube connected to the bottom of the soil column. Water content and temperature sensors were installed in the column to monitor the water content and the temperature. After the experiment, they modeled water and vapor fluxes with the numerical model SiSPAT (Simple soil-plant-atmosphere transfer model) (Braud et al., 1995).

Hernández-López et al. (2014) found differences between the observed and the simulated water profile, suggesting that the soil properties were modified by water and solute transport (Figure 1-1b). To obtain an agreement between the observed and the simulated water profile, they changed the soil properties defining arbitrary layers defined by electrical conductivity and water content profiles (Figure 1-1c, Figure 1-1d). Then, using three different layers they could represent correctly their experiment. These results suggest a change in soil properties as effect of evaporation fluxes.

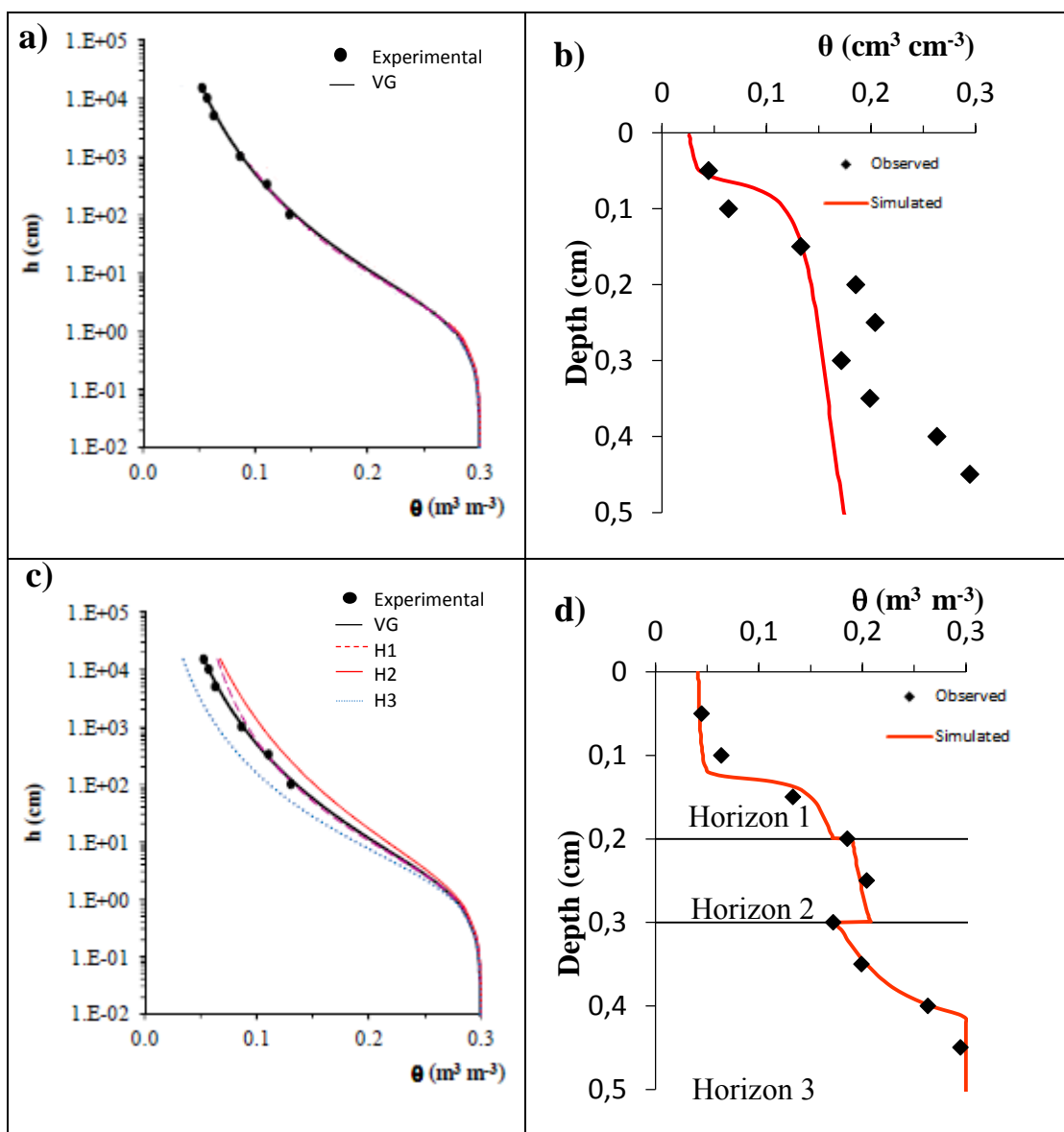


Figure 1-1: Results obtained by Hernandez-López et al. 2014 a) Observed (points) and estimated (line) water retention curve for original soil sample, b) observed (points) and simulated (line) water content profile after evaporation using SiSPAT model, c) Estimated water retention curves defined for stratified soil and d) observed and simulated water content profile using stratification.

Fujimaki et al. (2006) evaluated the effect of a salt crust on evaporation rates from a bare saline soil. They made evaporation experiments using different saline soil columns. Soil samples were initially saturated with ionic solutions and then were exposed to an infrared lamp to simulate the solar radiation. A constant matric potential was fixed at the bottom to maintain the soil surface wet and to assure that the matric potential does not affect evaporation fluxes. Figure 1-2 shows their result for two columns with the same soil and solute concentration. At the first stage, the observed evaporation rate decreases rapidly, and then the decrease is more gradual. This effect is due to a salt crust formed at the soil surface that increases the resistance to evaporation. They defined a numerical model to incorporate the salt crust effect (with r_{sc} in Figure 1-2) and predict correctly the experimental results. Figure 1-2 presents experimental and numerical results and shows that it is necessary to include the salt crust resistance effect to represent correctly the evaporation rates.

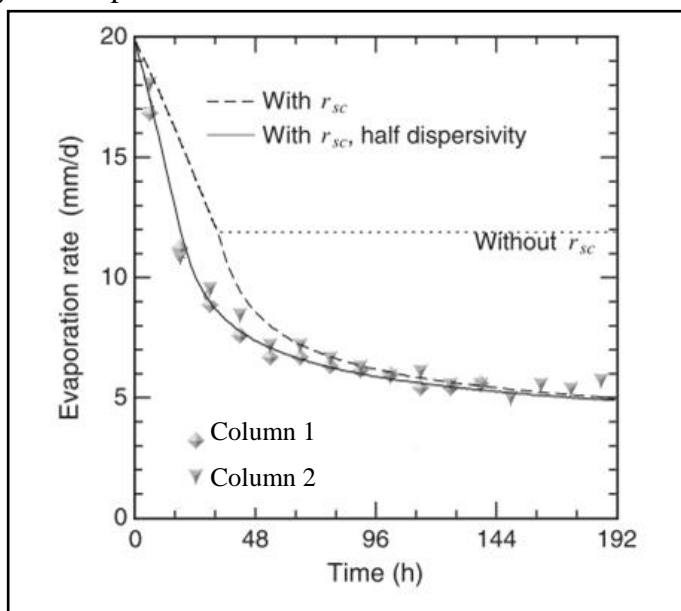


Figure 1-2: Experimental and simulated results of the evaporation rate from a saline soil. Numerical estimations improve when evaporation resistance of a salt crust at surface is considered (Modified from Fujimaki et al., 2006)

Gran et al. (2011) experimentally studied vapor flux and solute transport under evaporation conditions. Laboratory experiments consisted on initially saturated soil columns and an infrared lamp to represents solar radiation, which induces evaporation. They used two soils, sand and silt, and added ionic solutions to control soils salinity. Soil columns were weighted to determinate evaporation losses. Cumulative evaporation results (Figure 1-3) show that sand produces an initial evaporation rate that is higher than that of the silt. They suggested that this behavior is due to the higher hydraulic conductivities of sand. For both soils, the evaporation rate decreases with time because the surface becomes dry. Differences in high and low saline concentrations were found. For both soils, higher concentrations of halite or epsomite resulted in lower evaporation rates, which confirms that an increase on salts concentration decrease evaporation and suggest that different salts can produce different impacts on evaporation fluxes.

Figure 1-4 shows volumetric water content, salt concentrations and temperature profiles results reported by Gran et al. (2011) for sand and silt with halite. Sharp changes on the three profiles indicate the presence of the evaporation front near the surface (4 cm from the surface). Differences in water contents are principally due to the soil characteristics; silt has a homogeneous profile while sand presents a dry condition near the surface. Low and high concentrations of halite show a similar behavior. Moreover, solute concentration profiles show a sharp increase near the surface up to 4 cm, which demonstrates the transport of solute to the surface due to evaporation fluxes. Finally, temperature profiles show differences between sand and silt due to the thermal properties of each soil (Gran et al., 2011).

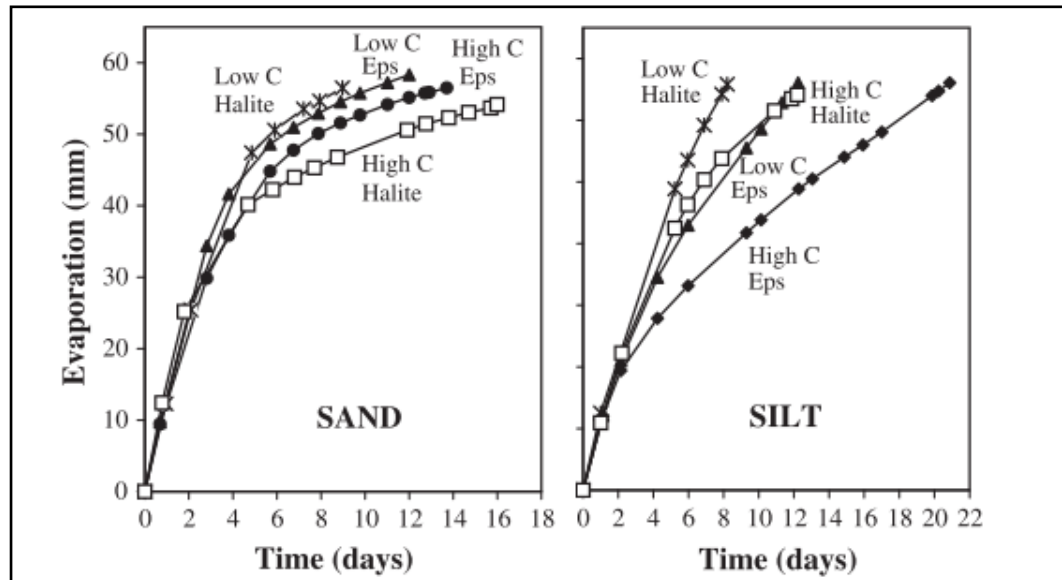


Figure 1-3: Cumulative evaporation in sand (left) and silt columns (right) with different salts types and concentrations. In both cases, evaporation is higher for lower salt concentrations (Gran et al, 2011).

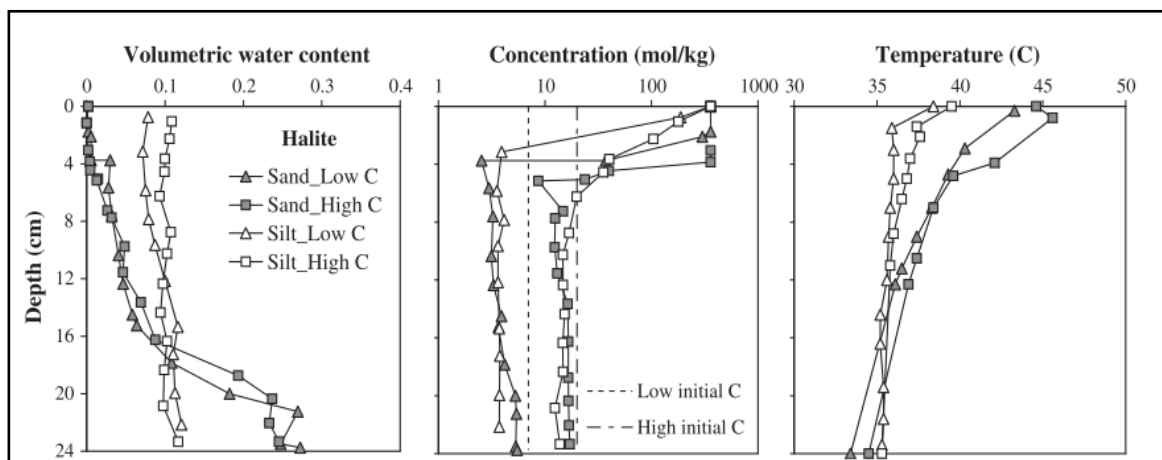


Figure 1-4: Water content, concentration and temperature profiles at the end of the halite experiment. Salt concentration increase at the surface, decreasing volumetric water content at this zone (Modified from Gran et al., 2011)

Zhang et al. (2014) developed a numerical model to predict evaporation rates from bare saline soils including the effect of salt precipitation. They defined evaporation stages based on the location of the vaporization plane and salt concentration profile and represented efflorescence and subflorescence salt precipitation. Efflorescence precipitation (i.e., a salt crust on the soil surface), results in a barrier that reduces evaporation fluxes. Subflorescence precipitation (i.e., beneath the soil surface), reduces the pore size and obstructs water vapor flow. Zhang et al. (2014) considered that salts change the soil porosity and water density. However, they did not consider changes on the water retention curve. Their main results are shown in Figure 1-5. The model shows a decrease in the evaporation fluxes caused by salt precipitation. These results were validated with the experimental data obtained from Gran et al. (2011) and Fujimaki et al. (2006). Also, they found a movement of the vaporization plane related with the water content and the evaporation rate (Figure 1-5a). When the soil had lost enough water (50% of saturation), the vaporization plane descends and the evaporation rate decreases to almost zero. Figure 1-5 b) shows the different evaporation stages: W1 corresponds to the first stage, where vaporization plane is located near the surface; W2 is defined as the stage where the vaporization plane is located away of the surface; S1 corresponds to a stage where the salt concentration is less than its solubility; S2 occurs when the salt concentration is higher than its solubility and efflorescence precipitation occurs; and in S3, salt concentration is also higher than its solubility but now subflorescence precipitation is observed.

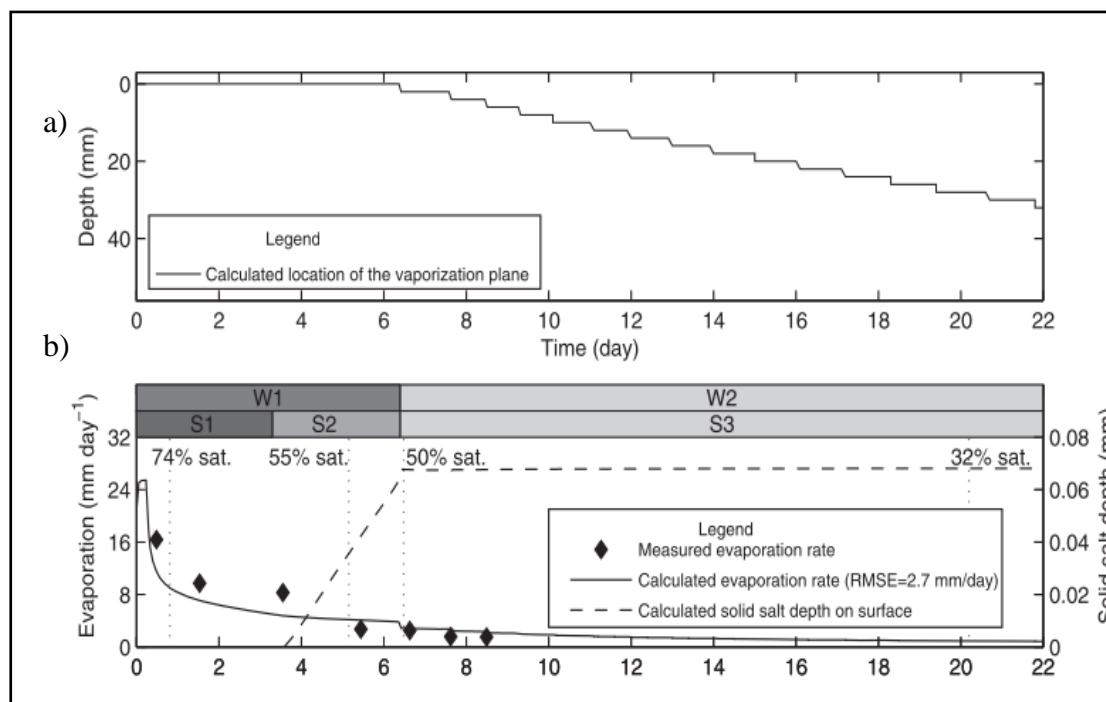


Figure 1-5: a) Change of the location of the vaporization plane; and b) Change of the evaporation rate and soil salt depth on soil surface. Vaporization plane decreases according to saturation. (Modified from Zhang et al., 2014)

On the other hand, Ciocca et al. (2014) evaluated the effect of the water retention curve on evaporation from arid soils. They evaluated the performance of the van Genuchten (1980) model (VG) on numerical simulations of drying soils. The VG model assumes no flow when water content is less than residual water content. That assumption eliminates vapor fluxes, which are predominant in moisture-limited regime and can reduce the estimated cumulative evaporation. Ciocca et al. (2014) proposed a modified van Genuchten model (MVG), which considers water retention as a function of the saturation, rather than of the effective saturation. This simple change permits that vapor fluxes continue removing soil water after liquid fluxes stop and the soil can dry below residual saturation. Ciocca et al. (2014) also evaluated the Webb (2000) model (WM), which modify the VG model in the dry range. Water retention curve defined for each

method are shown in Figure 1-6a. Numerical simulations realized with the three models shows that MVG and WM presents higher cumulative evaporations and differences are noticed when the evaporation rate decrease (Figure 1-6b).

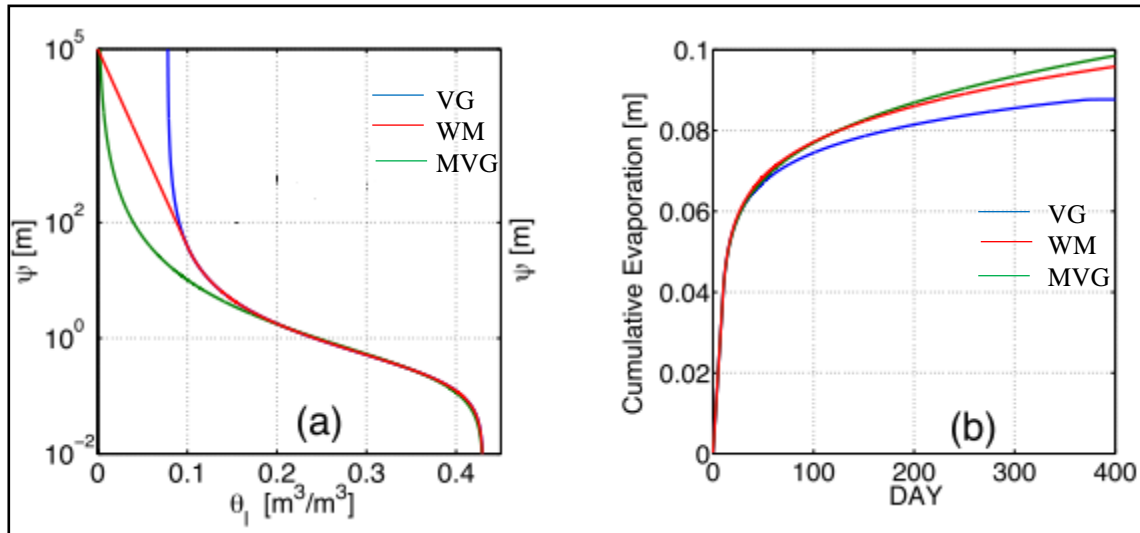


Figure 1-6: a) Water retention curves for loam. b) Cumulative evaporation for loam with three different models (Ciocca et al., 2014).

1.2.2 SAR index: Sodium adsorption ratio

Major ions that are present in arid zones interact in different ways with water (Hribar et al., 2002), and thus could affect evaporation rates. In these zones, the spatial distribution of salts is not homogeneous and depends on the geology and on the external processes in the region. Sodium (Na^+), calcium (Ca^{2+}) and magnesium (Mg^{2+}) are the three major cations present in these zones. There are zones with sodium predominance and others with calcium/magnesium predominance, thus it is necessary to evaluate the relationship between these ions. Typically, this relationship is defined using the sodium adsorption ratio (SAR) index (Sumner, 1993):

$$SAR = \frac{[Na^+]}{\left(\frac{[Ca^{2+}] + [Mg^{2+}]}{2}\right)^{0.5}} \quad (1.1)$$

where the brackets refer to molar concentration. SAR index is a direct way to measure soil sodicity, which is an important property that can affect the soils hydraulic properties (Oster and Shainberg, 2001; Suarez, 2001)

In the last two decades, there have been few studies of the effect of SAR on the hydraulic properties and water fluxes. Lima et al. (1990) studied the combined effect of SAR and salts molar concentration on the hydraulic properties of a loamy soil. They conducted an experiment that included analysis of water retention and hydraulic conductivity curves. They reported an increase on water retention capacity with an increase in sodium concentration or a decrease of solution concentration, but they did not determinate the isolated effect of the SAR index. Hydraulic conductivity curve results indicate that increasing salinity increases the nonlinearity of the $\log K(\theta)$ curve (Lima et al. 1990).

Suarez et al. (2006) studied the effect of SAR on water infiltration in natural soils. They evaluated two different soils (loam and clay) and five different SAR indexes (2, 4, 6, 8 and 10). In all cases, it was found that water infiltration decreases as the SAR index increases. For the loam soil the impact was identified above SAR=2 and for clays the impact was observed above SAR=4. It has been found that the SAR index has an effect on both infiltration rate and infiltration time.

1.3 Hypothesis

It is hypothesized that evaporation fluxes from saline soils are influenced by the soil SAR index. This dependency is mainly due to the effect of the SAR index on the soil water retention curve. Also, it is hypothesized that it is necessary to include salts concentration differences in stratified soils to estimate evaporation fluxes in saline soils.

1.4 Objectives

The main objective of this research is to evaluate the effect of the SAR index on evaporation fluxes from saline soils. The specific objectives of this investigation are:

- 1) To determine experimentally the effect of the SAR index on the soil hydraulic properties, i.e., water retention curve, $\theta(h)$, and hydraulic conductivity curve, $K(h)$.
- 2) To evaluate changes in cumulative evaporation from soils with different SAR indexes by means of numerical simulations.
- 3) To evaluate, using numerical modeling, changes in salts concentrations due to salts movement and precipitation/dissolution in the soil profile.
- 4) To evaluate, using numerical modeling, the effect of different SAR composition in the soil profile (stratified soil) on evaporation fluxes.

2 THEORY

Evaporation from saline soils includes transport of liquid water, vapor water, heat and solute (Gran et al., 2011; Zhang et al., 2014). In this section, the main transport equations that are involved in evaporation process are reviewed.

2.1 Liquid water and vapor flow

Liquid water and vapor flow in a porous medium is described by (Saito et al., 2006):

$$\frac{\partial \theta}{\partial t} = \frac{\partial}{\partial z} \left[(K + K_{vh}) \left(\frac{\partial h}{\partial z} \right) + (K_{LT} + K_{vT}) \frac{\partial T}{\partial z} \right] \quad (2.1)$$

where θ [L^3L^{-3}] is the total volumetric water content defined as the sum of the volumetric liquid and vapor content ($\theta = \theta_l + \theta_v$), t [T] is time, K [LT^{-1}] is the isothermal hydraulic conductivity of the liquid phase, K_{vh} [LT^{-1}] is the isothermal hydraulic conductivity of vapor phase, K_{LT} and K_{vT} [$L^2K^{-1}T^{-1}$] are the thermal hydraulic conductivity of the liquid and vapor phase, respectively, h [L] is the pressure head, z [L] is the spatial coordinate, and T [K] is the temperature.

To solve equation (2.1), it is necessary to define the soil water retention, $\theta(h)$, and hydraulic conductivity, $K(h)$, curves. The water retention curve determines the relationship between pressure head and water content and represents the soil capacity to hold water. The hydraulic conductivity curve represents the soil capacity to transport water under different pressure heads. The van Genuchten/Mualem models can be used to describe both curves (van Genuchten, 1980):

$$\theta_l(h) = \begin{cases} \theta_r + \frac{\theta_s - \theta_r}{(1 + |\alpha h|^n)^m} & h < 0 \\ \theta_s & h \geq 0 \end{cases} \quad (2.2)$$

$$K(h) = K_s S_e^l \left[1 - \left(1 - S_e^{\frac{1}{m}} \right)^m \right]^2 \quad (2.3)$$

where θ_s [L^3L^{-3}] is the saturated water content; θ_r [L^3L^{-3}] is the residual water content; α [L^{-1}] is the inverse of the air-entry pressure; l [-] is the pore-connectivity parameter, estimated as 0.5 (Mualem, 1976), n and m [-] are empirical parameters; K_s [LT^{-1}] is the saturated hydraulic conductivity; and S_e [-] is the effective saturation, defined as:

$$S_e = \frac{\theta - \theta_r}{\theta_s - \theta_r} \quad (2.4)$$

2.2 Heat transport

Heat transport coupled with vapor transport is described by (Saito et al., 2006):

$$C_p \frac{\partial T}{\partial t} + L_0 \frac{\partial \theta_v}{\partial t} = \frac{\partial}{\partial z} \left[\lambda(\theta) \frac{\partial T}{\partial z} \right] - C_w q \frac{\partial T}{\partial z} - L_0 \frac{\partial q_v}{\partial z} - C_v \frac{\partial q_v T}{\partial z} \quad (2.5)$$

where C_p, C_w and C_v [$ML^{-1}T^{-2}K$] are the volumetric heat capacities of the porous medium, liquid and vapor phase, respectively; q [LT^{-1}] is the liquid water flux density; T [K] is the soil temperature; L_0 [$MT^{-2}L^{-1}$] is the volumetric latent heat of vaporization of water; $\lambda(\theta)$ [$MLT^{-3}K$] is the soil apparent thermal conductivity; and q_v [LT^{-1}] is the vapor flux density.

The apparent thermal conductivity includes the thermal conductivity and the thermal dispersivity:

$$\lambda(\theta) = \lambda_0(\theta) + \beta_t C_w |q| \quad (2.6)$$

where β_t [L] is the thermal dispersivity and λ_0 [MLT^{-3}K] is the baseline thermal conductivity (in absence of fluid flow), defined as (Chung and Horton, 1987):

$$\lambda_0(\theta) = b_1 + b_2\theta + b_3\theta^{0.5} \quad (2.7)$$

where b_1 , b_2 and b_3 [$\text{MLT}^{-3}\text{K}^{-1}$] are empirical parameters.

2.3 Surface energy balance

To couple liquid water and vapor flow with heat transport, surface precipitation, irrigation, evaporation and heat fluxes are used as boundary conditions. The surface energy balance is used to calculate surface water and heat fluxes, and it is expressed as:

$$R_n - H - L_0E - G = 0 \quad (2.8)$$

where R_n [MT^{-3}] is the net radiation; H [MT^{-3}] is the sensible heat flux density; E [$\text{ML}^{-2}\text{T}^{-1}$] is the evaporation rate; and G [MT^{-3}] is the surface heat flux density (Saito et al., 2006).

2.4 Solute transport

This section reviewed the different mechanisms of solute transport. Solute transport may include salt movement and precipitation/dissolution processes.

2.4.1 Standard solute transport

One-dimensional nonequilibrium chemical transport of solutes in a variably saturated porous media is given by (Simunek et al., 2012)

$$\frac{\partial \theta c_i}{\partial t} + \frac{\partial \rho s_i}{\partial t} + \frac{\partial a_v g_i}{\partial t} = \frac{\partial}{\partial z} \left(\theta D_i^w \frac{\partial c_i}{\partial z} \right) + \frac{\partial}{\partial z} \left(a_v D_i^g \frac{\partial g_i}{\partial z} \right) - \frac{\partial q c_i}{\partial z} \quad (2.9)$$

where c_i [ML^{-3}], s_i [MM^{-1}] and g_i [ML^{-3}] are solute i concentrations in the liquid, solid and gaseous phases, respectively; a_v [L^3L^{-3}] is the air content; D_i^w [L^2T^{-1}] is the dispersion coefficient for the liquid phase and D_i^g [L^2T^{-1}] is the diffusion coefficient for the gas phase.

The interactions between the liquid and solid (adsorbed) concentrations can be assumed to occur in equilibrium, and the following adsorption isotherm is used to describe these interactions (Šimůnek et al., 2013):

$$s_i = \frac{K_1 c_i^\beta}{1 + \eta c_i^\beta} \quad (2.10)$$

where K_1 [-], η [-] and β [-] are empirical parameters.

On the other hand, equilibrium interaction between the solution and gas concentrations is assumed and it is described as a linear expression:

$$g_i = K_2 c_i \quad (2.11)$$

where K_2 [-] is an empirical constant.

2.4.2 Equilibrium chemistry .

A one-dimensional advective-dispersive chemical transport equation is used for each aqueous species (Ions Ca^{2+} , Na^+ , Mg^{2+} , K^+ , HCO_3^- , Cl^- and SO_4^{2-}) (Suarez & Simunek, 1997):

$$\frac{\partial \theta c_k}{\partial t} + \rho \frac{\partial \bar{c}_k}{\partial t} + \rho \frac{\partial \hat{c}_k}{\partial t} = \frac{\partial}{\partial z} \left[\theta D \frac{\partial c_k}{\partial z} - q c_k \right] \quad k = 1, \dots, N. \quad (2.12)$$

where c_k [ML^{-3}] is the total dissolved concentration of the aqueous species k , \bar{c}_k [MM^{-1}] is the total sorbed concentration of the aqueous component k , \hat{c}_k [MM^{-1}] is the total nonadsorbed concentration of aqueous component k , ρ [ML^{-3}] is the bulk density of the medium, D [L^2T^{-1}] is the dispersion coefficient (which includes diffusion and hydrodynamic dispersion coefficients) and N is the number of aqueous species.

The equilibrium chemical reactions included are complexation, precipitation/dissolution, cation exchange and adsorption (Suarez & Simunek, 1997). Precipitation/dissolution processes is expressed by a kinetic model. To describe cation exchange between the solid phase and the solution, the model uses a Gapon expression (White and Zelazny, 1986).

$$K_{ij} = \frac{\bar{c}_i^{z_i^+} (\bar{c}_j^{z_j^+})^{\frac{1}{z_j}}}{\bar{c}_j^{z_j^+} (\bar{c}_i^{z_i^+})^{\frac{1}{z_i}}} \quad (2.13)$$

where z_i and z_j are the valences of species i and j , respectively.

3 MATERIALS AND METHODS

3.1 Determination of soil properties

This section describes the experimental methods used to determine the soil hydraulic and thermal properties, which were used utilized later in the numerical simulations.

3.1.1 Samples preparation

The soil used in this research is a fine-homogeneous sand. Eight similar samples were extracted and mixed with ionic solutions with SAR values of 0, 5, 10 and 15. Ionic solutions were prepared adding sodium chloride (NaCl) and calcium chloride (CaCl₂) to distilled water (Table 3-1).

Table 3-1: Ionic solutions composition.

Salts concentration [g/L]				
Salt	Solution 1	Solution 2	Solution 3	Solution 4
NaCl	1.75	1.75	1.75	0
CaCl ₂	0.44	0.99	3.99	0
SAR index	15	10	5	0

Two parts of each solution were mixed with one part of soil and left for four days to equilibrate (Lima et al., 1990). Two soil replicates were made for each SAR. After the experiments, each soil sample was analyzed using the TMECC 04.14 and 04.12 B method (Thompson et al., 2001) to determinate Na⁺, Ca⁺ and Mg⁺ ions concentration. These concentrations were used to calculate the SAR index of each sample.

3.1.2 Hydraulic properties

The water retention curve of each sample, $\theta(h)$, was determined using Tempe cells (1400 Tempe Pressure Cell, Soilmoisture Equipment Corp., Santa Barbara, CA), to study the effect of the SAR index on the water retention curve. This method was selected because it has smaller errors for coarse soils (Solone et al., 2012).

Figure 3-1 shows the experimental assembly, which consists in four weighable cells connected to an air compressor and valve that allows a controlled release of air at a specific pressure into the cells. Thus, the cells are under the same pressure at any time.

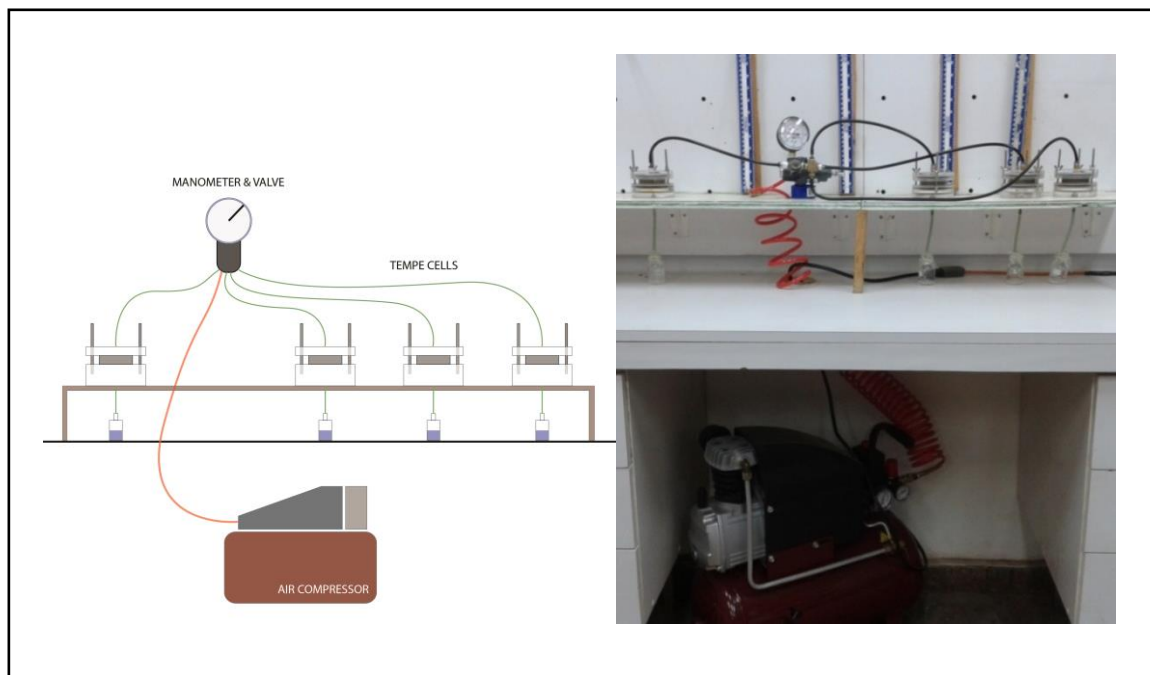


Figure 3-1: Experimental setup - Water retention curve

By applying a certain pressure to the soil, the water drains until an equilibrium state between the applied pressure and the water retained in the pores of the soil is

achieved. Once this state is reached, the cells are weighed and the volumetric moisture content is calculated according to:

$$\theta(h) = \frac{V_w(h)}{V_t} = \frac{M_w(h)}{\rho_w * V_t} = \frac{M_t(h) - M_s}{\rho_w * V_t} \quad (2.14)$$

where $\theta(h)$ [L^3L^{-3}] is the soil water content; h [L] is the manometric pressure; $V_w(h)$ [L^3] is the volume of water in the soil at a pressure h ; ρ_w [ML^{-3}] is the water density; $M_t(h)$ and $M_w(h)$ [M] are the sample and water mass at pressure h , respectively; M_s [M] is the dry soil mass; and V_t [L^3] is the total sample volume.

Saturated hydraulic conductivity was determined using a constant head permeameter, for the samples with different SAR. Figure 3-2 shows the experimental setup.

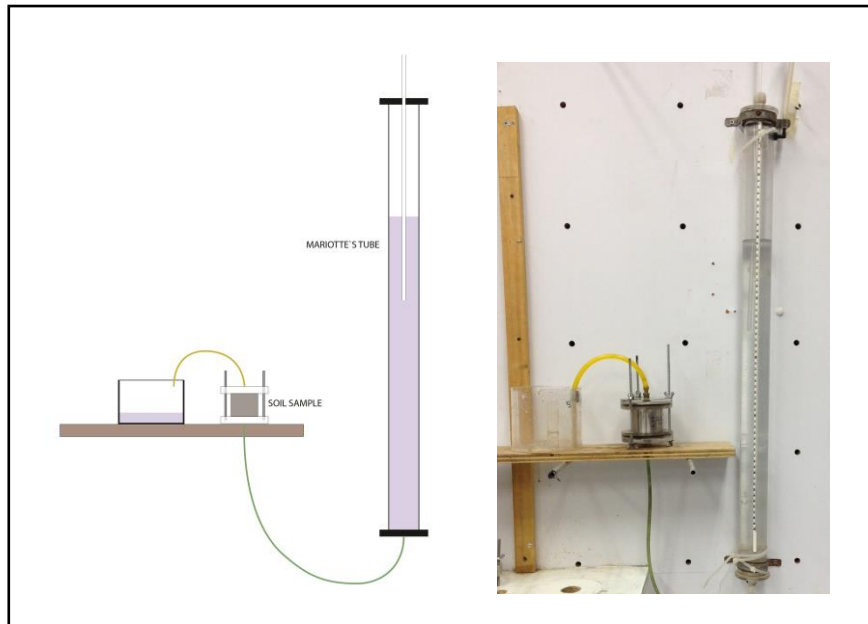


Figure 3-2: Experimental setup - Constant head permeameter

3.1.3 Thermal properties

Soil thermal properties were determined using a thermal properties analyzer (KD2 pro, Decagon devices, Inc., USA), which determines the thermal conductivity, K_{Th} [LT^{-3}]; thermal diffusivity, D_{Th} [L^2T^{-1}] and specific heat C [$L^2M^{-1}T^{-2}$]. Simultaneously, a time domain reflectometry (TDR) sensor was used to determine the soil water content (Figure 3-3). To determine the Chung and Horton equation parameters (Eq. 2.7), the thermal conductivity was measured for different water contents to obtain a relationship between thermal conductivity and water content. Then, the parameters of the Chung and Horton (1987) model (Eq. 2.7) were fitted by least-squares adjustment to represent the experimental data.



Figure 3-3: Experimental setup to determine the thermal properties as a function of soil water content.

3.2 Model simulations

This section explains the simulations performed with HYDRUS 1D. Different numerical simulations were used to evaluate the SAR effect on evaporation fluxes. In the following sections are explain the different simulations types.

3.2.1 Numerical model: HYDRUS 1D

HYDRUS 1D is one dimensional finite elements model that simulate the movement of water, heat and multiple solute in porous media. This model resolve the transport equations reviewed in section 2, and it has been widely used for simulating the movement of water flow in variably saturated porous media (Ramos et al., 2011; Singh et al., 2011; Selim et al., 2013; Suárez et al., 2013) .

This model incorporates the effect of water flow on heat and solute transport, but not the inverse relation.

HYDRUS 1D incorporates two ways of modeling solute transport: 1) the UNSATCHEM module, which includes precipitation/dissolution reactions (solve equations of section 2.4.2); and 2) the standard solute transport which not (solve equations of section 2.4.1). To include precipitation/dissolution reactions we used the UNSATCHEM module. However, it is not compatible with the surface energy balance equation (equation 2.8) which is necessary to couple water flow and heat transport. Thus, we first used the standard solute transport module to determine evaporation fluxes when water and heat transport are coupled, and these results were used as boundary conditions for the simulations with the UNSATCHEM module to evaluate the possible salts concentration changes on soil profile as a result of evaporation fluxes.

Water flow boundary conditions

To solve equation (2.1) a known initial distribution of the pressure head in the whole profile must be defined:

$$h(z, t) = h_i(z), \quad t = t_0 \quad (2.14)$$

where h_i [L] is the specific value of pressure as a function of depth (z), respectively. System-independent and/or system-dependent boundary conditions can be defined. The system-independent boundary conditions are:

$$\begin{aligned}
 h(z, t) &= h_0(t), & z = 0 \text{ (surface) or } z = L \text{ (bottom)} \\
 -K \left(\frac{\partial h}{\partial z} + \cos\alpha \right) &= q_0(t), & z = 0 \text{ or } z = L \\
 \frac{\partial h}{\partial z} &= 0, & z = 0
 \end{aligned} \tag{2.15}$$

where h_0 [L] and q_0 [LT^{-1}] are the specified values of the pressure head and the soil water flux at the boundary, respectively. One of the system-dependent boundary conditions available in Hydrus 1D considers the soil-air interface, which is exposed to atmospheric conditions. This boundary condition defines a potential fluid flux across the soil surface that depends exclusively by external (ambient) conditions and the actual flux, which depends on the water content near the surface. The absolute value of the surface flux is limited by the following conditions:

$$\begin{aligned}
 \left| -K \frac{\partial h}{\partial x} - K \right| &\leq E & z = L \\
 h_A &\leq h \leq h_S & z = L
 \end{aligned} \tag{2.16}$$

where E [LT^{-1}] is the potential rate of evaporation or infiltration and h_A [L] and h_S [L] are minimum and maximum allowed pressure head at the soil surface, respectively.

3.2.2 Evaporation from soils with different SAR

The evaporation process in a soil profile was simulated using a soil column with constant water table level. To evaluate the effect of SAR on evaporation fluxes, soils with different hydraulic properties were used under the same environmental conditions. The hydraulic properties were chosen to represent the effect that the SAR index has on the water retention curve.

A soil profile of 200 cm was modeled; Figure 3-4 presents the conceptual model of the simulations. The total simulation time was 60 days. As water flow surface boundary condition, it was used a conditions which use atmospheric data to calculate water fluxes and heat transport at the surface. This condition couple water and vapor fluxes, and heat transport (Eq. 2.16). Meteorological data from Pampa del Tamarugal, Chile, was used in the simulations. These data were collected between March and April of 2006 from the National system of information of air quality (SINCA, 2006), which includes temperature, precipitation, net radiation, wind speed, and relative humidity. The collected data is characteristic of arid zones as exhibit extreme temperatures at day and night, very low precipitations, high radiation and low relative humidity. At the bottom of the soil profile, we used a constant positive pressure to fix a constant water table of 100 cm. As initial conditions, we considered a soil profile in equilibrium (linear distribution of pressure head). A uniform initial temperature and solute concentration were utilized. The standard solute transport module was used. As solute transport boundary conditions, we used zero concentration flux at both the top and the bottom of the column. Finally, as heat transport boundary conditions, we used the surface energy balance (explained before) at the surface and zero thermal gradient at the bottom. The solute transport and reaction parameters are described in Table 3-2.

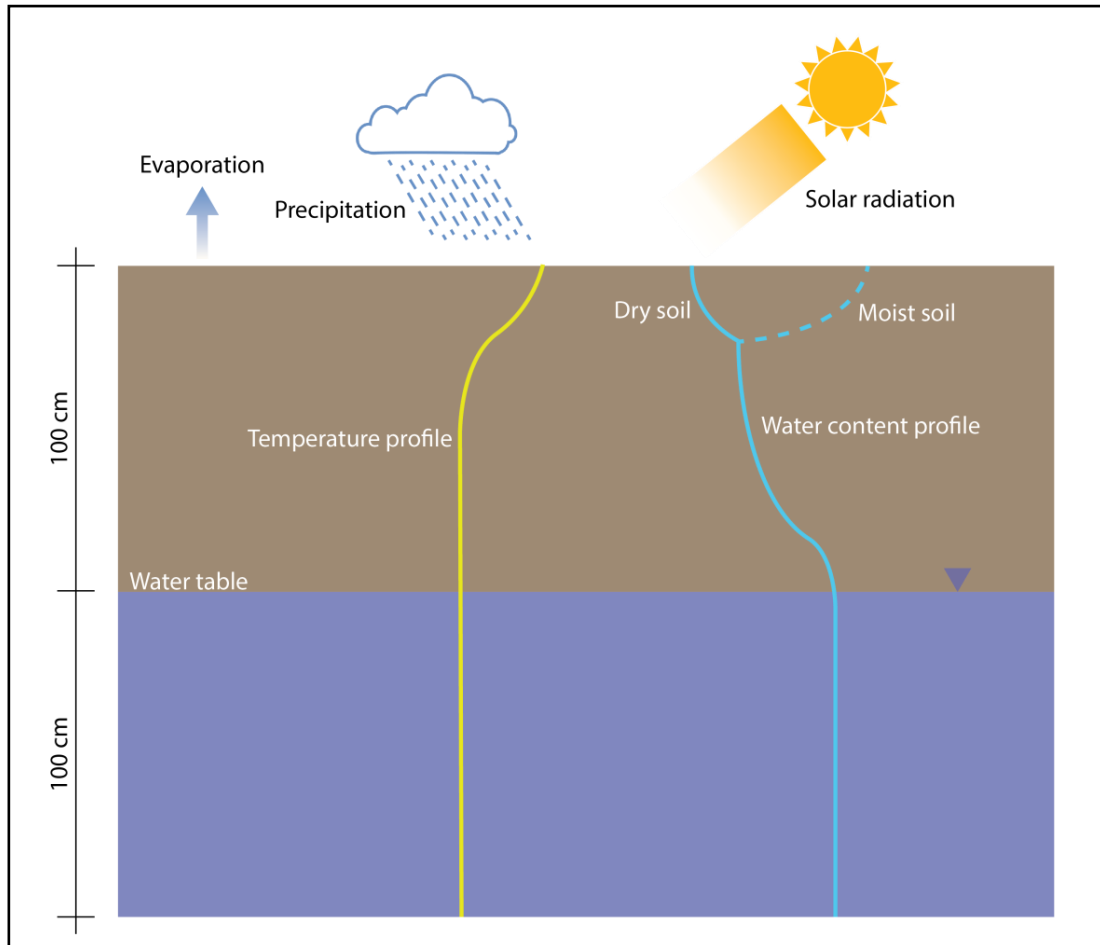


Figure 3-4: Conceptual model.

Table 3-2: Solute transport and reaction parameters used on numerical simulation.

Parameter	Value	Unit
Bulk density, ρ^a	1.3	g/cm^3
Longitudinal dispersivity ^b	20	cm
Adsorption isotherm coef. k_s^c	2	cm^3/g
Adsorption isotherm coef. β^c	1.2	-

^a Calculated as an average of typical values for sand (Assouline et al, 2006; Ramos et al., 2011). ^b Calculated as an average of typical values for sand (Gelhar et al., 1992). ^c A Freundlich isotherm was assumed.

Three different water retention curves were used to represent three soils with different SAR, which allows comparing evaporation fluxes for each simulation. Water retention curves were obtained from the experimental work.

In the simulations explained above, the water table level was selected arbitrarily. To evaluate if this value has an impact on the evaporation results, the same simulation was run in two soils with four different water table levels; 50, 75, 100 and 125 cm.

3.2.3 Effect of evaporation on salts concentration

The effect of evaporation fluxes on salt movement, precipitation or dissolution was also evaluated. The conceptual model of this simulation is the same as that shown in the previous simulation (Figure 3-4), but in this case the UNSATCHEM module was used to represent accurately the salt behavior (e.g., precipitation/dissolution reactions). The boundary conditions used at top of the soil column was the atmospheric conditions including the evaporation results obtained from the previous simulations. These evaporation fluxes were used because the UNSATCHEM module is not compatible with the surface energy balance equation (Section 2.3). In this simulation, a soil with SAR 3.7

was used. The others initial and boundary conditions were the same than those presented previously, and the water table level was fixed at a depth of 100 cm.

3.2.4 Effect of soil stratification on evaporation fluxes

Previous researchers have reported non uniform salt concentrations on soil profile as effect of water movement (Gran et al. 2011; Hernández-López et al. 2014; Zhang et al. 2014). As result of evaporation, precipitation/dissolution reactions can occur and soil composition will change. Then, according with the results of salt movement obtained previously, a stratified soil with hydraulic properties dependent on the SAR index was defined. Initial and boundary conditions are the same those previous simulations, and the conceptual model is shown in Figure 3-5.

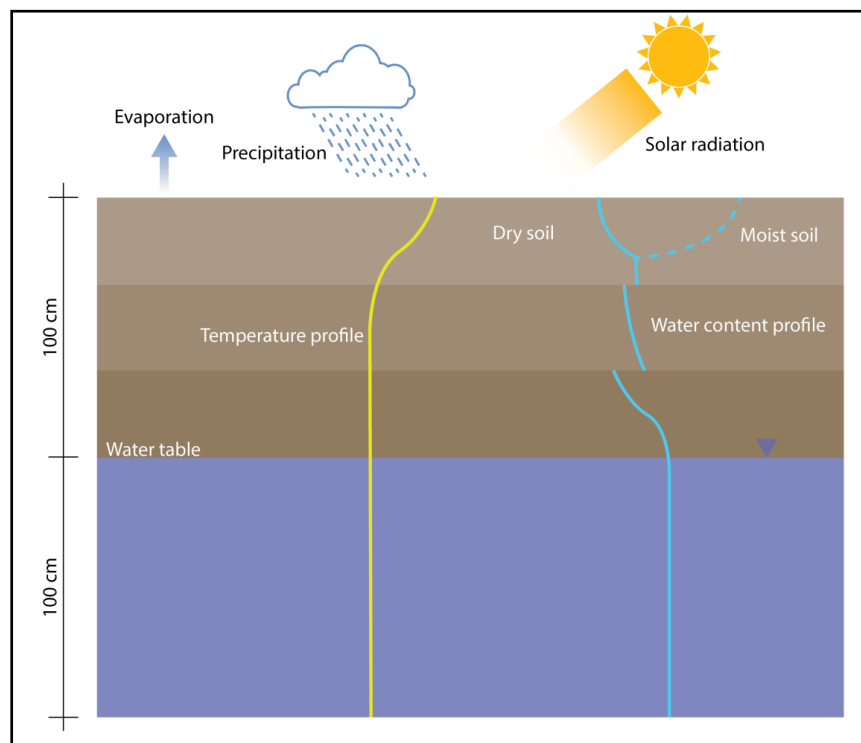


Figure 3-5: Conceptual model for a stratified soil.

4 RESULTS AND DISCUSSION

This section presents the results of the experimental work and numerical modeling.

4.1 Soil properties

4.1.1 Hydraulic properties

The chemical analysis of the soils samples showed five different soils with SAR indexes of 5.4, 3.84, 3.73, 2.9 and 2.5. Figure 4-1 presents the experimental data and the estimated water retention curves for each sample using the RETC model (van Genuchten et al., 1991) to fit the van Genuchten parameters to the experimental points. An increase in the SAR value increases the water retention capacity of the soil for a fixed pressure. This increase is explained by the sodium concentration disperses the soil particles, which decreases the pore size thus increasing the capillary forces (Lima et al., 1990; Rengasamy & Olsson, 1991; Bourrie, 2014). This behavior has been observed by other authors (Lima et al., 1990). The SAR effect decrease near the extreme of the curve, that is, the SAR does not affects the residual and the saturated water content.

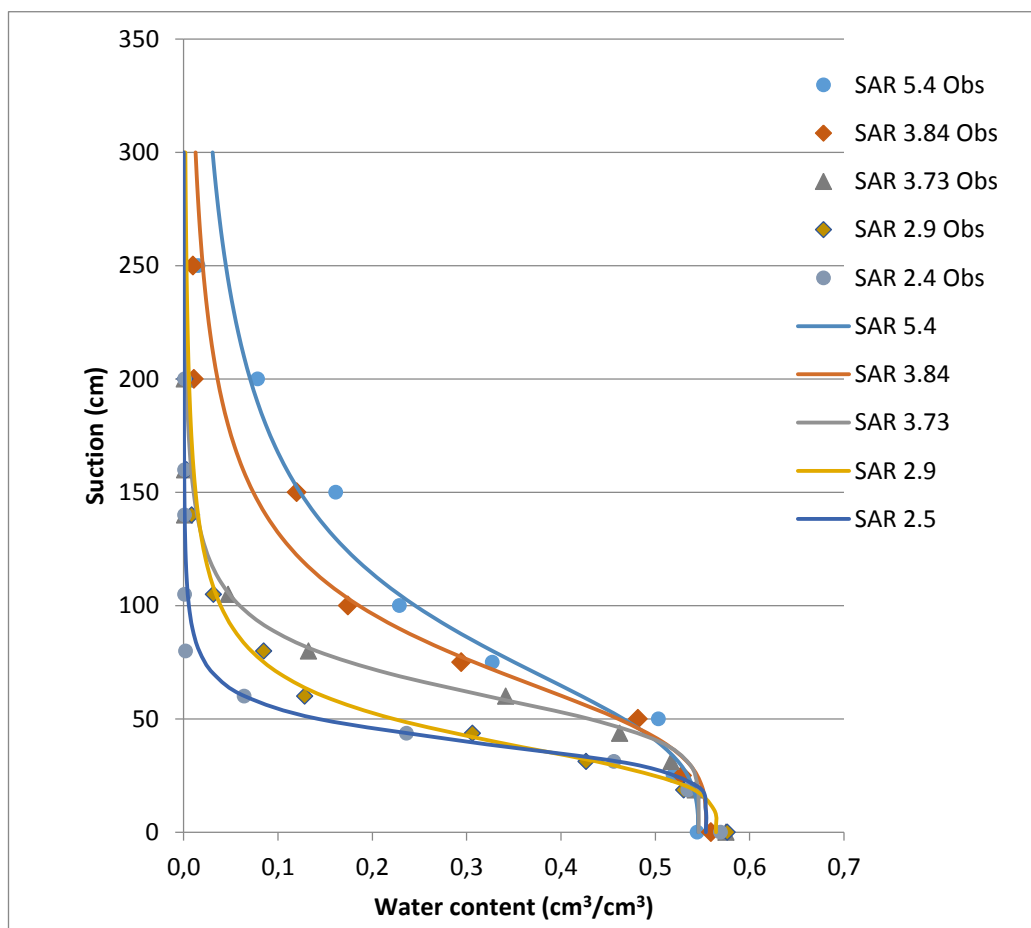


Figure 4-1: Observed (points) and estimated (lines) water retention curve for saline soils with different SAR. Results indicate that an increase in the SAR increases the water retention capacity of the soil for a fixed pressure.

Table 4-1 shows the soil estimated water retention parameters. The saturated water content varied less than 5% in the soils with different SAR. These variations are attributable to measurement errors. The residual water content did not show any variation as a consequence of the SAR. The inverse of the air-entry pressure (α) showed a significant increase as the SAR index decrease, with differences up to 90% compared

to the soil with less SAR. This difference corresponds to a decrease in the air entry pressure from 76.9 cm to 40 cm, this behavior is consistent with that reported by Lima et al. (1990). The parameter n shows an inverse relation with the SAR index, except for the soil with SAR 2.9. An important increase of the parameter n is observed between SAR 3.84 and SAR 3.73. Finally, the parameter m follows the same behavior than parameter n because it is calculated as a function of n ($m = 1 - \frac{1}{n}$).

Table 4-1: Soil water retention parameters obtained by using the van Genuchten's equation (1980).

SAR	$\theta_r \left[\frac{\text{cm}^3}{\text{cm}^3} \right]$	$\theta_s \left[\frac{\text{cm}^3}{\text{cm}^3} \right]$	$\alpha \text{ [cm}^{-1}\text{]}$	n	m	R^2
5.40	0.0	0.545	0.013	3.111	0.68	0.998
3.84	0.0	0.553	0.014	3.608	0.72	0.998
3.73	0.0	0.545	0.016	5.384	0.81	0.997
2.90	0.0	0.564	0.025	3.834	0.74	0.997
2.50	0.0	0.553	0.025	5.950	0.83	0.999

Saturated hydraulic conductivity results for the three measured soils are shown in Table 4-2. Similar results are obtained for three soils. There is no effect of SAR variation in saturated hydraulic conductivity for this soil. This result is explained because the distilled water used in the permeameter wash the salts in the soil. To improve these results it is necessary use water with the same SAR of the studied soil in the permeameter.

Table 4-2: Hydraulic conductivity for three soils with different SAR. Results indicate no significant differences between these three soils.

	SAR 2.9	SAR 3.84	SAR 5.4
$K_s \left[\frac{cm}{s} \right]$	$4,7 * 10^{-3}$	$3,5 * 10^{-3}$	$5,5 * 10^{-3}$

4.1.2 Thermal properties

Figure 4-2 shows the thermal conductivity curve estimated with the Chung and Horton (1987) model and the experimental data. Empirical parameters obtained with the least square method and fitted coefficients are shown in Table 4-3. The estimated thermal conductivity curve presents a slightly decrease towards the saturated zone, but this no affect the modelling results.

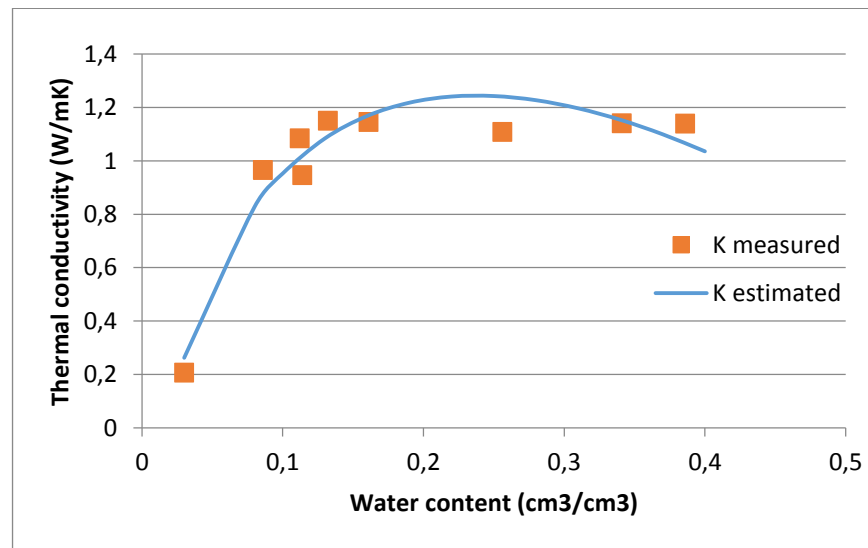


Figure 4-2: Thermal conductivity curve. Measured (points) and estimated (line) thermal conductivities for different water content values.

Table 4-3: Chung and Horton parameters and fitted coefficient.

$b1 [W/mK]$	$b2 [W/mK]$	$b3 [W/mK]$	R^2
-1.116	-9.931	9.684	0.93

4.2 Model simulations

4.2.1 Evaporation from soils with different SAR

Figure 4-3 shows the cumulative evaporation after 60 days for three different soils with SAR values of 5.4, 3.84 and 3.73. Soils with higher SAR present higher cumulative evaporation with differences up to 68% after 60 days of simulation. Results show higher differences between soil with SAR 3.84 and 3.73, which are directly related to the differences in soil water retention curves estimated in the laboratory. Cumulative evaporation is greater for a soil with higher SAR because this soil has more water retention capacity and keeps the soil wetter near the surface than a soil with lower SAR. This behavior it is observed in the water content profile. Figure 4-4 shows the water content profile for the three soils after 60 days with a water table of 100 cm depth. A slight increase of water content is observed in the three cases due to the last time of simulation corresponds to midnight of the day 60.

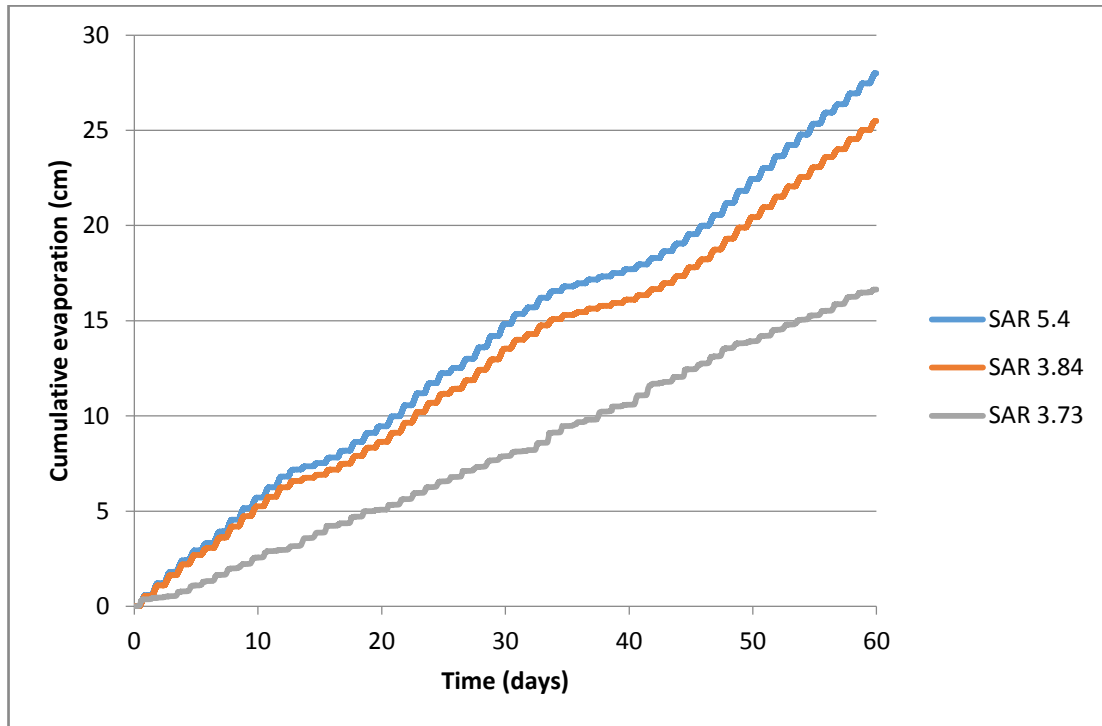


Figure 4-3: Estimated cumulative evaporation for three soils with different SAR after 60 days of simulation. A soil with higher SAR presents higher cumulative evaporation than other soils with lower SAR index.

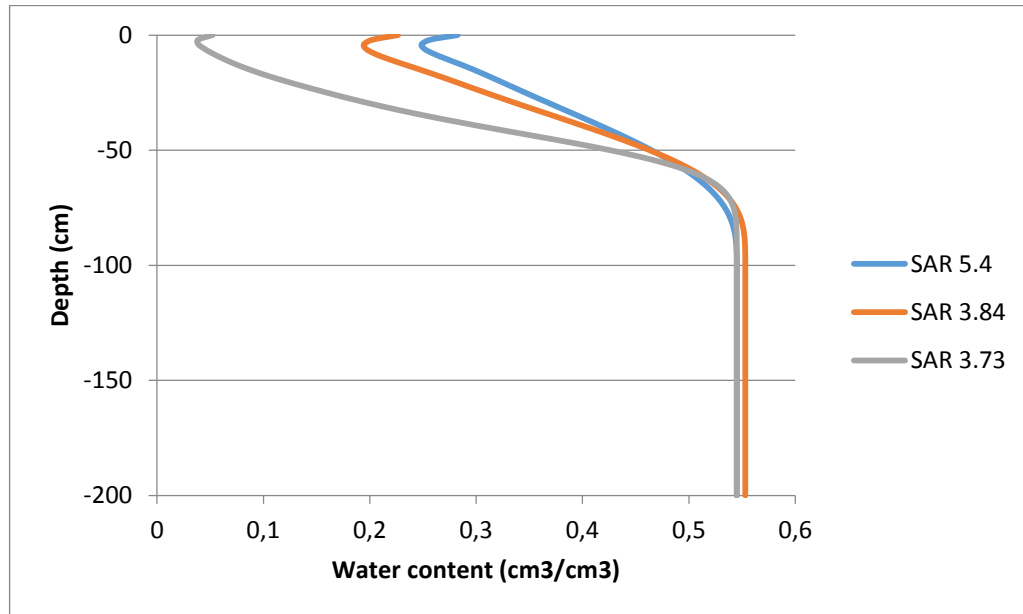


Figure 4-4: Water content profile for three soils with different SAR after 60 days. The soil with higher SAR presents a wetter profile than the other soils under the same conditions.

Table 4-4 shows cumulative evaporation after 60 days simulated for four different water table levels. These simulations indicate the influence of water table in the effect of SAR on evaporation fluxes. If water table level is deeper, cumulative evaporation differences between two soils with different SAR increase dramatically. For a very shallow water table of 50 cm, difference between a soil with SAR 3.84 and other one with SAR 5.4 is negligible, but if water table is at 125 cm, the difference increase to 58%. These results are expected because there is less water available and changes in water retention curve have a higher impact (Ciocca et al., 2014). As was explained in section 1.1, when water table level is near to surface and soil is wet, evaporation mainly depends on external conditions. As in these simulations the atmospheric conditions were

the same, there are not differences in cumulative evaporation. But when the soil is drier and there is less water available, evaporation fluxes depends on soil hydraulic properties, which are modified by variations in the SAR.

Table 4-4: Cumulative evaporation after 60 days for different scenarios; two soils with different SAR and four water table levels. Differences between the two soils increase when the water table gets deeper.

Water table depth (cm)	Cumulative evaporation (cm)		Percentage difference (%)
	SAR 3.83	SAR 5.4	
50	29.75	29.85	0.3
75	29.10	29.50	1.3
100	25.49	28.00	9.8
125	15.63	24.76	58.4

4.2.2 Effect of evaporation on salts concentration

Figure 4-5 shows the SAR index distribution in the soil profile after 7 days of simulation. As initial condition, a uniform soil with SAR 3.73 was used. Results show an increase of the SAR near the surface. An increase in sodium and calcium concentrations was observed, these results are in agreement with to previous investigations (Gran et al, 2011; Zhang et al., 2014).

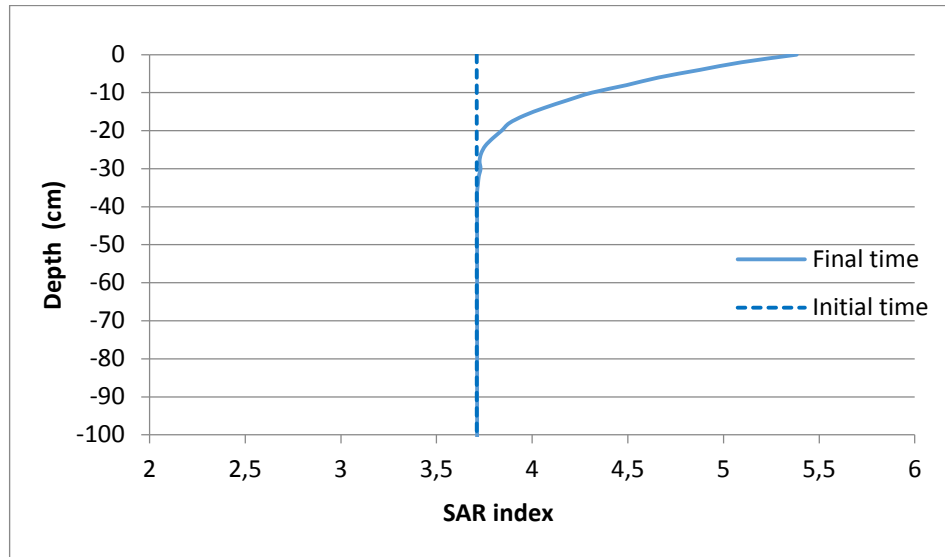


Figure 4-5: SAR index distribution after 7 days of simulation. The SAR index increases near the surface as a result of evaporation fluxes.

4.2.3 Effect of soil stratification on evaporation fluxes

According to the SAR distribution shown in Figure 4-5, the SAR index increases near the surface as a result of evaporation fluxes. Therefore, a stratified soil with three layers was defined. The first layer corresponds to a soil with SAR 5.4 and has a thickness of 12 cm, second layer is a soil with SAR 3.84 and 12 cm thickness and third layer corresponds to the original soil with SAR 3.73 and 176 cm thickness. The following results were obtained assuming that the water table level is at 100 cm depth. Figure 3-5: Conceptual model for a stratified soil. shows the conceptual model for the stratified soil with three different layers.

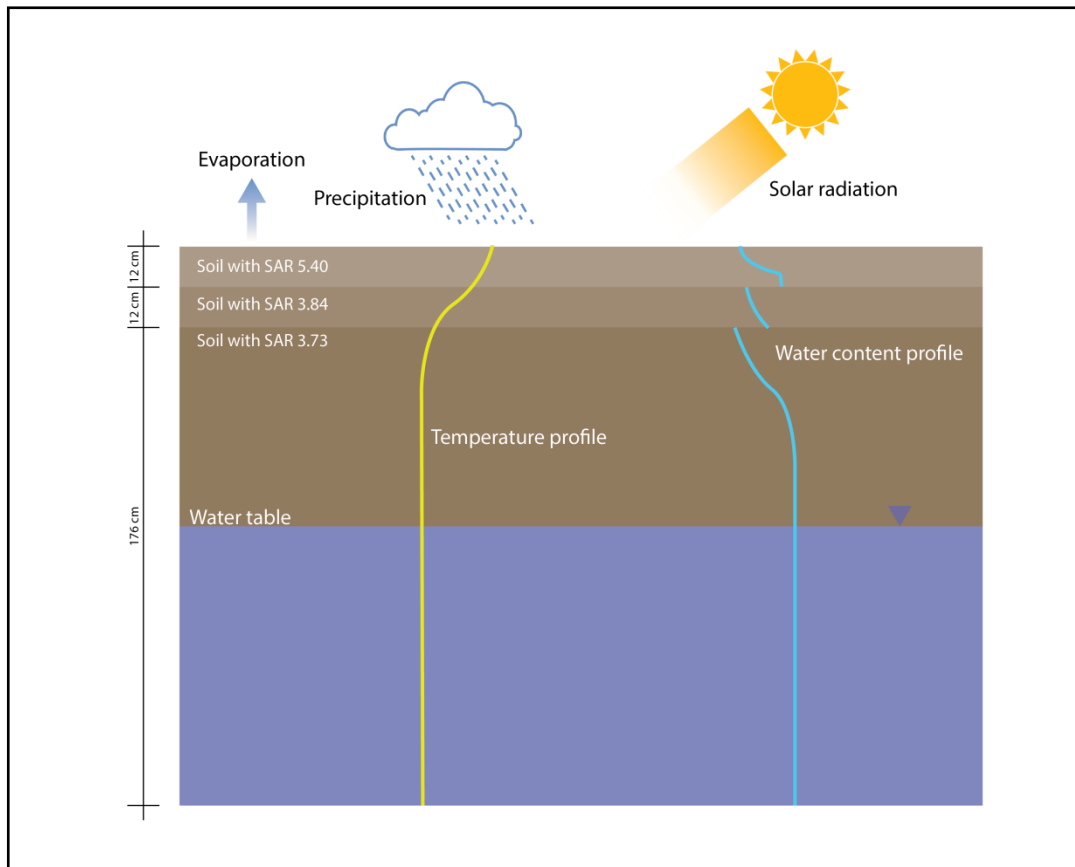


Figure 4-6: SAR distribution for the stratified soil.

Figure 4-7 shows the cumulative evaporation of both the original soil with SAR 3.73 and the stratified soil with a higher SAR at the soil surface. Stratified soil presents greater cumulative evaporation than the uniform soil. This result is expected because soil with SAR 5.4 and soil with SAR 3.84 have a higher cumulative evaporation than soil with SAR 3.73. The curve of cumulative evaporation for the stratified soil is almost equal to a uniform soil with SAR 5.4. This indicates that first layer has the major influence on evaporation.

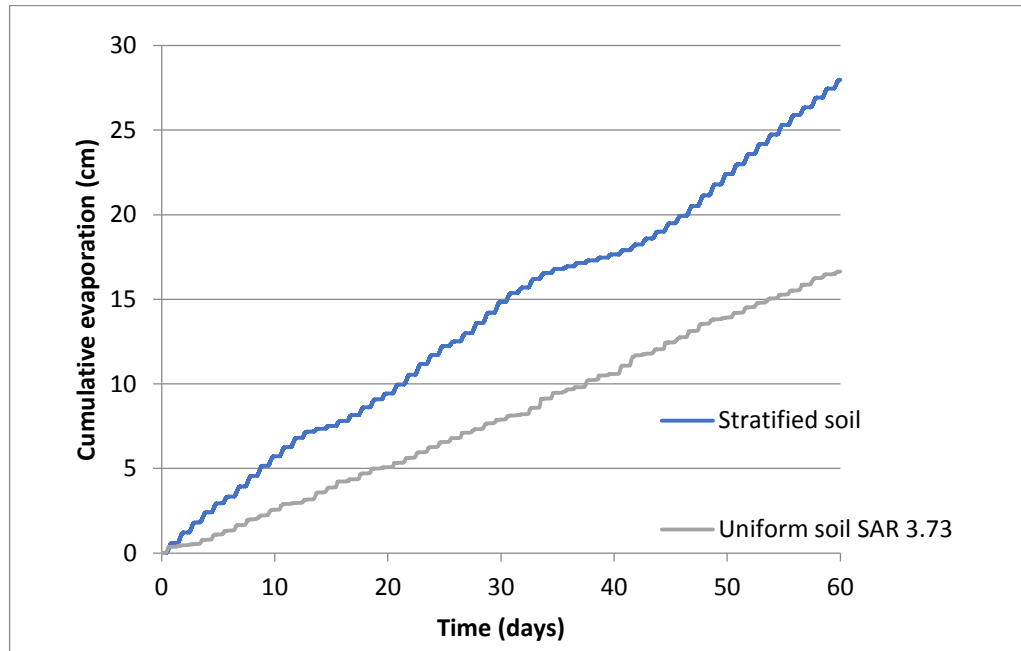


Figure 4-7: Estimated cumulative evaporation for a uniform and stratified soil. The stratified soil presents greater evaporation than the uniform soil.

To analyze the influence of the first layer thickness on evaporation fluxes, a stratified soil with two layers was defined; the first layer corresponds to a soil with SAR 5.4 and second layer is a soil with SAR 3.73. The thicknesses of both layers were different for each simulation to evaluate its impact on evaporation. Figure 4-8 shows the cumulative evaporation of the stratified soil as a function of the first layer thickness. When the thickness of the first layer increases, the cumulative evaporation of the stratified soil approaches the cumulative evaporation of a uniform soil SAR 5.4. For instance, when the thickness of the first layer is around 6 cm, the cumulative evaporation of the stratified and the uniform soils differ in less than 1%.

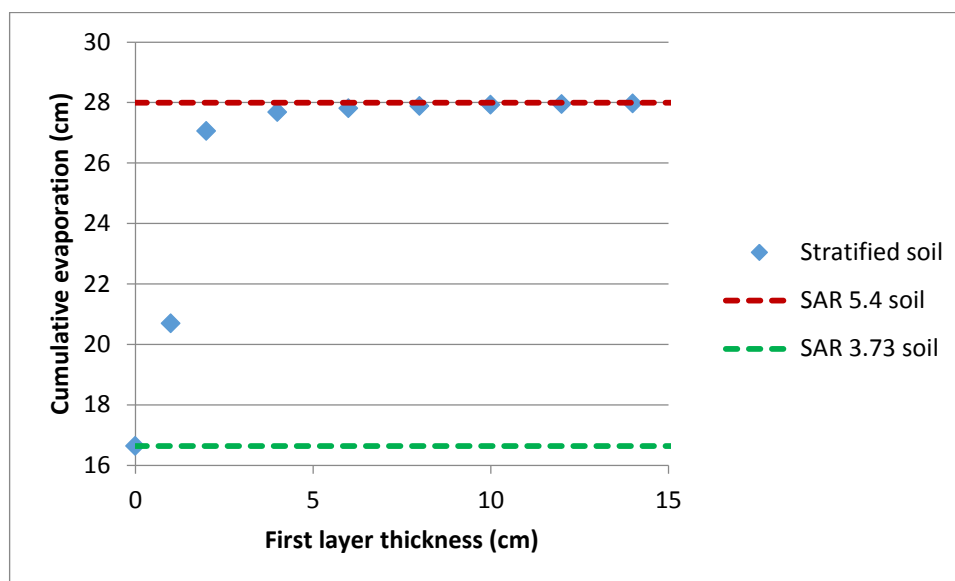


Figure 4-8: Cumulative evaporation as a function of the first layer thickness of a stratified soil after 60 days of simulation (points). The dashed lines indicate the cumulative evaporation for a uniform soil with SAR 3.73 (green) and 5.4 (red). When the first layer thickness increases, evaporation from the stratified soil is similar to a uniform soil with the same SAR of first layer.

5 CONCLUSIONS

In arid zones, evaporation from shallow groundwater is an important component of the water balance. Evaporation is a complex process, which under dry conditions, directly depends of soil hydraulics properties. Thus it is necessary to understand how these properties affect the evaporation fluxes.

This research evaluated the effect of the SAR index on evaporation fluxes from shallow groundwater. The effect of SAR on soil hydraulic properties was analyzed experimentally and these results were applied on numerical simulations of evaporation from a soil profile. The main conclusions of this work are presented below.

5.1 SAR effect on soil hydraulic properties

The water retention curve was determined experimentally for five soils with SAR values between 2.5 and 5.4. Variations in salt concentrations changed the soil water retention curve. Under the same pressure, a soil with higher SAR presented more water retention capacity than a soil with lower SAR. This increase in the water retention capacity is due to the ability of the sodium to disaggregate the soil particles, reducing the pore size, and increasing the capillary forces. Changes were not significant for residual and saturated water content. Also, soils with higher SAR present a higher air entry pressure with differences up to 50%. The hydraulic conductivity was determined using a constant head permeameter and no significant differences were found for the soils under investigation because the water used in the permeameter was distilled water.

5.2 SAR effect on evaporation

Numerical simulations were used to evaluate the impact of water retention curve variations on evaporation fluxes. Results show that a soil with higher SAR presents more cumulative evaporation than a soil with lower SAR. Differences in cumulative

evaporation increase when water table is deeper. For a wet soil profile with a water table of 25 cm depth, the gap between a soil with SAR 5.4 and SAR 3.8 are negligible but for a water table of 125 cm depth the difference increases over 58%. These variations occur because in wet soils evaporation depends mostly on ambient conditions, but when the soil is drier, evaporation also depends on hydraulic properties. Evaporation is higher in soils with higher SAR because they soils have greater water retention capacity and keep the surface wetter than other soils. This phenomenon was observed on the water content profile.

In saline soils, evaporation fluxes cause changes in salts distribution in soil profile making them non uniform. Numerical simulations results show a salt accumulation near surface due to ascendant water and vapor fluxes. Changes in salts distribution modify the SAR index in the soil profile. The SAR index increases at the surface. The new SAR distribution, modify the soil profile and results in heterogeneous hydraulic properties. The stratified soil structure presents different evaporation rates under the same conditions than a soil with uniform SAR. It was observed a predominance of the first layer hydraulic properties on the evaporation fluxes. Results show that evaporation mainly depends on the hydraulic properties of the first 6 cm of soil for a water table of 100 cm depth.

5.3 General conclusions

Evaporation fluxes in saline soils cause a continuous movement of salts. This variation in salt concentrations changes the water retention curve of the soil making it non uniform. Modifying the water retention curve affects the evaporation rates from the groundwater. This relationship between salt concentration and water retention capacity should be incorporated in models to have a better representation of the real processes of evaporation. As a future work, it is necessary develop a numerical relation between the SAR index and the water retention curve.

REFERENCES

- Assouline, S., Tyler, S. W., Tanny, J., Cohen, S., Bou-Zeid, E., Parlange, M. B., & Katul, G. G. (2008). Evaporation from three water bodies of different sizes and climates: Measurements and scaling analysis. *Advances in Water Resources*, 31(1), 160–172
- Bittelli, M., Ventura, F., Campbell, G. S., Snyder, R. L., Gallegati, F., & Rossi, P. (2008). Coupling of heat, water vapor, and liquid water fluxes to compute evaporation in bare soils. *Journal of Hydrology*, 362(3-4), 191–205.
- Boulet, G., Braud, I., & Vauclin, M. (1997). Study of the mechanisms of evaporation under arid conditions using a detailed model of the soil–atmosphere continuum. Application to the EFEDA I experiment. *Journal of Hydrology*, 193(1-4), 114–141
- Bourrie, G. (2014). Swelling clays and salt-affected soils: demixing of Na/Ca clays as the rationale for discouraging the use of sodium adsorption ratio (SAR). *Eurasian Journal of Soil Science*, 3, 245-253.
- Braud, I., Dantas-Antonino, A.C., Vauclin, M., Thony, J.L. & Ruelle, P. (1995). A simple soil-plant-atmosphere transfer model (SiSPAT) development and field verification. *Journal of Hydrology*, 166, 213-250.
- Chung, S. O. & Horton, R. (1987). Soil heat and water flow with partial surface mulch. *Water Resources Research*, 23(12), 2175-2186.
- Ciocca, F., Lunati, I. & Parlange, M. B. (2014). Effects of the water-retention curve on evaporation from arid soils. *Geophysical Research Letters*, 41, 9, 3110-3116
- Decagon Devices, Inc. GS3: Water Content, EC and Temperature Sensors: Operator's manual. Decagon Devices, Inc. Pullman WA 99163, 1-23
- Decagon Devices, Inc. KD2 Pro thermal properties analyzer: Operator's manual. Decagon Devices, Inc. Pullman WA 99163, 1-63
- Fujimaki, H., Shimano, Inoue, M., Nakane, K. (2006). Effect of a salt crust on evaporation from a bare saline soil. *Vadose Zone Journal*, 5, 1246-1256
- Gardner, W.R. & Hillel, D. (1962). The relation of external evaporative conditions to the drying of soils. *Journal of Geophysical Research*, 67, 4319-4325.

Gran, M., Carrera, J., Massana, J., Saaltink, M. W., Olivella, S., Ayora, C., & Lloret, A. (2011). Dynamics of water vapor flux and water separation processes during evaporation from a salty dry soil. *Journal of Hydrology*, 396(3-4), 215–220.

Gran, M., Carrera, J., Olivella, S., & Saaltink, M. W. (2011). Modeling evaporation processes in a saline soil from saturation to oven dry conditions. *Hydrology and Earth System Sciences*, 15(7), 2077–2089.

Han, J. & Zhou, Z. (2013). Dynamics of soil water evaporation during soil drying: Laboratory experiment and numerical analysis. *The Scientific World Journal*, 2013, 1-10.

Hernández, M. F. (2012). *Evaluación Experimental y Numérica de la Evaporación desde Aguas Subterráneas Someras. Aplicación a Suelos Salinos de la Cuenca del Salar de Huasco*. Pontificia Universidad Católica de Chile.

Hernández-López, M.F., Gironás, J., Braud, I., Suárez, F., Muñoz, J.F. (2014). Assessment of evaporation and water fluxes in a column of dry saline soil subject to different water table levels. *Hydrological Processes* 28(10). 3655-3669

Hribar, B., Southall, N. T., Vlachy, V., & Dill, K. A. (2002). How Ions Affect the Structure of Water. *American Chemical Society*, (11), 12302–12311.

Idso, S. B., Reginato, R. J. Jackson, R. D., Kimball, K.B., Nakayama, F. S. (1974). Three stages of drying in a field soil. *Soil Sci. Soc. Am. Proc.*, 38, 831-837.

Johnson, E., Yáñez, J., Ortiz, C., & Muñoz, J. (2010). Evaporation from shallow groundwater in closed basins in the Chilean Altiplano. *Hydrological Sciences Journal*, 55(4), 624–635.

Kondo, J., Saigusa, N., & Sato, T. (1990). A parametrization of evaporation from bare soil surfaces. *Journal of Applied Meteorology*, 29, 385–389.

Lima, L. A. ., Grismer, M. E. ., & Nielsen, D. R. . (1990). Salinity effects on Yolo Loam Hydraulic Properties. *Soil Science*, 150(1), 451–458.

Mualem, Y. (1976). A new model for predicting the hydraulic conductivity of unsaturated porous media. *Water Resources Research*, 12, 513-522.

- Nassar, I. N., & Horton, R. (1999). Salinity and compaction effects on soil Water Evaporation and Water and Solute Distributions. *Soil Science Society of America Journal*, 63, 752–758.
- Oster, J. & Shainberg, I. (2001). Soil responses to sodicity and salinity: Challenges and opportunities. *Australian Journal of Soil Research*, 39, 1219-1224.
- Penman, H. L. (1948). Natural evaporation from open water, bare soil, and grass. *Proc. R. Soc. London*, A193, 120-145.
- Qiu, G. Y., & Ben-Asher, J. (2010). Experimental Determination of Soil Evaporation Stages with Soil Surface Temperature. *Soil Science Society of America Journal*, 74(1), 13.
- Ramos, T. B., Šimůnek, J., Gonçalves, M. C., Martins, J. C., Prazeres, a., Castanheira, N. L., & Pereira, L. S. (2011). Field evaluation of a multicomponent solute transport model in soils irrigated with saline waters. *Journal of Hydrology*, 407(1-4), 129–144.
- Rengasamy, P. & Olsson, K., A. (1991). Sodicity and soil structure. *Australian Journal of Soil Research*, 29, 935-952.
- Rose, D. A. A., Konukcu, F. B., & Gowing, J. W. A. (2005). Effect of watertable depth on evaporation and salt accumulation from saline groundwater. *Australian Journal of Soil Research*, 43, 565–573.
- Sailor, D. J. & Hagos, M. (2011). An update and expanded set of thermal property data for green roof growing media. *Energy and Buildings*, 43, 9, 2298–2303.
- Saito, H., Šimůnek, J., & Mohanty, B. P. (2006). Numerical Analysis of Coupled Water, Vapor, and Heat Transport in the Vadose Zone. *Vadose Zone Journal*, 5(2), 784–800.
- Salas, J. (2000). Hidrologia de zonas aridas y semiaridas. *Ingenieria Del Agua*, 7(4), 409–429.
- Shah, N., Nachabe, M., & Ross, M. (2007). Extinction depth and evapotranspiration from ground water under selected land covers. *Ground Water*, 45(3), 329–38.
- Selim, T., Berndtsson, R., & Persson, M. (2013). Simulation of soil water and salinity distribution under surface drip, 362(April), 352–362

Šimůnek, J., Sejna, M., Saito, H., Sakai, M., & van Genuchten, M. T. (2013). Version 4.16 March 2013. Riverside, CA.

Šimůnek, J., Sejna, M., & van Genuchten, M. T. (2012). The UNSATCHEM Module

Singh, P. N., Wallender, W. W., & Asce, M. (2011). Effects of Soil Water Salinity on Field Soil Hydraulic Functions. *Journal of Irrigation and Drainage Engineering*, 137(5), 295–304

Sistema nacional de información de calidad del aire (SINCA). [On line] <http://sinca.mma.gob.cl/index.php/estacion/index/id/5>

Solone, R., Bittelli, M., Tomei, F., & Morari, F. (2012). Errors in water retention curves determined with pressure plates: Effects on the soil water balance. *Journal of Hydrology*, 470-471, 65–74

Springer, G., Wienhold, B. J., Richardson, J. L., & Disrud, L. a. (1999). Salinity and sodicity induced changes in dispersible clay and saturated hydraulic conductivity in sulfatic soils. *Communications in Soil Science and Plant Analysis*, 30(15-16), 2211–2220.

Suarez, D. L., & Simunek, J. (1997). UNSATCHEM: Unsaturated Water and Solute Transport Model with Equilibrium and Kinetic Chemistry. *Soil Science Society of America Journal*, 61, 1633–1646

Suárez, D. (2001). Sodic soil reclamation: Modelling and field study. *Australian Journal of Soil Research*, 39, 1225-1246

Suárez, D., Wood, J. & Lesch, S. (2006). Effect of SAR on water infiltration under a sequential rain-irrigation management system. *Agricultural Water Management*, 86, 1-2, 150-164.

Sumner, M., E. (1993). Sodic soils: New perspectives. *Australian Journal of Soil Research*, 31, 683-750.

Thompson, W., Leege, P., Millner, P., & Watson, M. (2001). Test Methods for the Examination of Composting and Compost.

Ullman, W. J. (1985). Evaporation rate from a salt pan: Estimates from chemical profiles in near-surface groundwaters. *Journal of Hydrology*, 79(3-4), 365–373.

Van Genuchten, M. T. (1980). A Closed-form Equation for Predicting the Hydraulic Conductivity of Unsaturated Soils 1. *Sci. Soc. Am. J.*, 44, 892–898.

Van Genuchten, M. T., Leij, F. J., & Yates, S. R. (1991). The RETC Code for Quantifying the Hydraulic Functions of Unsaturated Soils. Riverside, CA: U. S. Salinity Laboratory.

Webb, S. W. (2000). A simple extension of two-phase characteristic curves to include the dry region, *Water Resour. Res.*, 36(6), 1425–1430.

White, N. & Zelazny, L. W. (1986). Charge properties in soil solids. *Soil Physical Chemistry*.39-81.

Xue, Z., & Akae, T. (2010). Effect of Soil Water Content and Salinity on Daily Evaporation from Soil Column, 6(8), 576–580

Zhang, C., Li, L., & Lockington, D. (2014). Numerical study of evaporation-induced salt accumulation and precipitation in bare saline soils: Mechanism and feedback. *Water Resources Research*, 50, 1–23